$C^{12}(x,xn)C^{11}$ and $Al^{27}(x,x2pn)Na^{24}$ Cross Sections at High Energies*

Walter E. Crandall,† George P. Millburn, Robert V. Pyle, and Wallace Birnbaum†

Radiation Laboratory, University of California, Berkeley, California

(Received August 1, 1955)

The $C^{12}(x,xn)C^{11}$ and $Al^{27}(x,x2pn)Na^{24}$ cross sections were measured for protons (105 to 350 Mev), deuterons (85 to 190 Mev), and alpha particles (380 Mev) by using a $4\pi\beta$ counter to determine the absolute disintegration rate and measuring the incident flux with a Faraday cup. The absolute value of the $C^{12}(p,pn)C^{11}$ excitation function was found to be 13% lower than the value previously published for these energies, and was found to be constant between 200 and 350 Mev. The new value of this reaction cross section removes some of the discrepancies between p-p scattering cross sections measured elsewhere and those measured at Berkeley, and affects other experiments that use the reaction as a proton flux monitor. The other cross sections are in reasonable agreement with values determined by comparable methods.

The relative excitation functions for $C^{12}(d,dn)C^{11}$ and $C^{12}(He^3,He^3n)C^{11}$ reactions were also measured by a stacked-foil technique using end-window counters. These were normalized to absolute values from the 4π counter data for deuterons.

I. INTRODUCTION

ABSOLUTE cross sections for reactions producing C^{11} and Na^{24} from bombardment of C^{12} and Al^{27} with high-energy particles have been determined for protons of 105 to 350 Mev, deuterons of 85 to 190 Mev, and alpha particles of 380 Mev, by use of the external beams of the 184-inch cyclotron. Many of the excitation functions have been determined previously, some by essentially the same technique used in this experiment,[1-5] but because of the importance of these reaction cross sections for beam monitoring[6-8] it was decided to redetermine the absolute values separately. An important feature of the experiment was the nearly concurrent measurement of all the cross sections, which should help insure high accuracy of the ratios.

The method involved absolute determination of the number of particles impinging on the targets by use of a Faraday cup, and absolute determination of the disintegration rate by use of a 4π, constant-flow, methane proportional counter calibrated against a similar instrument of the National Bureau of Standards,[9] and against β-γ coincidence counting.

Corrections for self-absorption in the foils were empirically determined.

Besides a desire to redetermine the absolute cross sections in view of recent advances in absolute β counting, an incentive for the experiment was the discrepancy in the shape of the $C^{12}(p,pn)C^{11}$ excitation function near 350 Mev as reported by two different groups.[1,2] Two methods of degrading the proton energy were used to explore the reasons for the discrepancy. The same technique was applied to the $C^{12}(d,dn)C^{11}$ excitation function near the maximum available energy (190 Mev). The $C^{12}(\alpha,\alpha n)C^{11}$ and $Al^{27}(x,x2pn)Na^{24}$ reaction cross sections were measured only for the maximum particle energies.

In an experiment which preceded the bulk of the work being reported, the relative excitation functions for the $C^{12}(d,dn)C^{11}$ and $C^{12}(He^3,He^3n)C^{11}$ reactions were measured by a stacked-foil technique. An end-window counter was used in these experiments and the results were normalized from the 4π counter data for deuterons. Although the precision of these measurements was low compared with the other cross sections, the values were included for completeness.

The following discussions relate only to the techniques and procedures used in the 4π counter experiments; discussion of the end-window counter data is reserved for the end of the paper.

II. EXPERIMENTAL PROCEDURE

A. Beam Characteristics and Monitoring

A plan view of the cyclotron is shown in Fig. 1. Most of the measurements were made with the scattered external beam which emerged from the magnetic deflectors, passed over the proton probe cart, through the premagnet collimator, through the steering magnet, and then through the 48-inch collimator and into the experimental area (cave). All the beams used were monoergic to within 1%.

[1] Aamodt, Peterson, and Phillips, Phys. Rev. **88**, 739 (1952); W. W. Chupp and E. M. McMillan, Phys. Rev. **72**, 873 (1947).

[2] Warshaw, Swanson, and Rosenfeld, Phys. Rev. **95**, 649(A) (1954).

[3] M. Lindner and R. N. Osborne, Phys. Rev. **91**, 1501 and 342 (1953).

[4] Stevenson, Hicks, and Folger, Phys. Rev. (to be published).

[5] Batzel, Crane, and O'Kelley, Phys. Rev. **91**, 939 (1953).

[6] L. Marquez, Phys. Rev. **88**, 225 (1952); Phys. Rev. **86**, 405 (1952).

[7] E. Belmont and J. M. Miller, Phys. Rev. **95**, 1554 (1954).

[8] p-p and p-d scattering cross sections affected by the change in the $C^{12}(p,pn)C^{11}$ excitation curve are: Birge, Kruse, and Ramsey, Phys. Rev. **83**, 274 (1951); Oxley, Shamberger, and Towler, Phys. Rev. **78**, 326 (1950); **84**, 1262 (1951); **85**, 416 (1952); **85**, 1024 (1952); Cassels, Pickavance, and Stafford, Proc. Roy. Soc. (London) **214**, 262 (1952). Other experiments affected include: J. W. Meadows, Phys. Rev. **91**, 885 (1953); K. Strauch and J. A. Hoffman, Phys. Rev. **86**, 563 (1952); **90**, 449 (1953); L. Marquez and I. Perlman, Phys. Rev. **81**, 953 (1951).

[9] We are indebted to Dr. H. H. Seliger of the Radioactivity Section of the National Bureau of Standards for his assistance in providing us with sources previously calibrated in their $4\pi\beta$ counter.
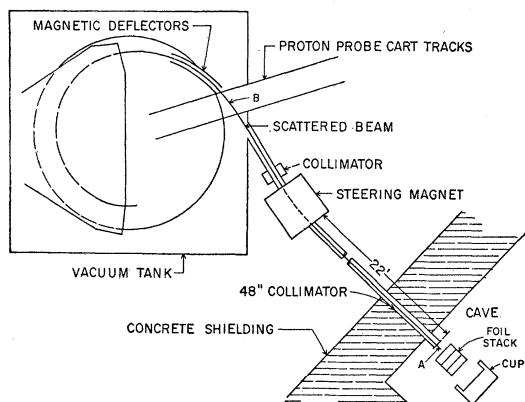
FIG. 1. Plan view of the cyclotron showing the path of the scattered beam. Absorbers for the "good geometry" experiments were placed on the proton probe cart and interposed in the scattered beam at position B; the steering-magnet current was then adjusted so that only particles of the proper energy entered the cave.

The beam was monitored by a Faraday cup.[1] The signal from the cup was led to one of several low-leakage Fast condensers which had been calibrated against a similar condenser measured by the National Bureau of Standards to within 0.1%.[10] Measurements made with different condensers showed excellent agreement. The voltage on the condenser was measured by a 100% inverse-feedback integrating electrometer and a Speedomax recorder, which were calibrated against a Rubicon potentiometer to within 0.1%.

The charge collected by the Faraday cup must be related to the number of particles that passed through the target foils. Factors that must be considered in the measurement of the beam include secondary emission (electrons or heavy charged particles) from the face of the cup, high-energy secondary particles emitted forward from the thin foil (0.005 in. Be-Cu) in the face of the vacuum housing, loss of charge by conduction through the cup supports and residual gas in the cup housing, and the relative area of the foils and the cup compared to the spatial distribution of the beam.

Previous experience with the Faraday cup used in this experiment showed that a thin foil biased to ±300 volts had a negligible effect on the collection characteristics of the cup when it was used in the experimental area shown in Fig. 1. Presumably the stray magnetic field (~25 gauss) in this area was more effective than a biasing voltage applied to the foil. An additional magnetic field ·(~100 gauss) produced no observable change in the collection efficiency of the cup. Thus secondary emission from the face of the cup was not an important source of error.

Teflon insulators were used throughout the collection system with a resulting time constant for the entire system of many days. The gas pressure in the cup

chamber had to be increased to more than 100 microns before ionization of the gas by the beam was observable. Conduction losses were minimized by maintaining the cup close to ground potential through the action of the feedback amplifier.

The spatial distribution of the beam was investigated by exposing an array of plastic scintillators (CH) diametrically across the beam. The C^{11} activity was essentially constant near the center and then dropped rapidly to less than 10^{-4} of the activity of the central region. If the activity in the region beyond the rapid falloff is attributed to a neutron flux, then the correction (1.25%) for the portion of the charged particle beam collected by the cup that did not pass through the target foils was almost precisely canceled by the correction for the neutron flux.

The largest correction to the Faraday cup readings resulted from the high-energy electrons emitted from the vacuum-housing foil.[11]

The number of electron collisions in a copper foil of thickness t mg/cm^2 is determined by the Rutherford scattering cross section,

$$N_e = \int_{x_1}^{t} dx \int_{0}^{\theta_{max}} 1.37 \times 10^{-4} \frac{z^2 t \, d \cos\theta}{\beta^4 \cos^3\theta}$$

per incident particle of charge z with velocity βc. The maximum energy of the electrons is $(4m/M)E$ for an incident particle of mass M and energy E (nonrelativistically). Not all the electrons escape from the foil because of their finite range and multiple scattering. By neglecting the latter effect and assuming the electron range to be well defined (i.e., a sharp drop to zero intensity at a unique thickness), one may calculate a maximum correction. In Table I the results of such calculations are tabulated assuming the electron ranges to be 1.0, 0.7, and 0.5 of the extrapolated ranges.[12] The curves for number vs absorber thickness may be approximated by straight lines, so the mean range is half the extrapolated range. Therefore we have chosen to use the calculations for half the extrapolated range, and, in order to take into account the multiple scattering, we have arbitrarily applied only one-half the calculated correction. We assign an uncertainty in the beam monitoring equal to the applied correction.

B. Degradation of Particle Energy

Carbon absorbers placed in front of the target foils in the path of the beam were used to degrade the incident energy. The particle current that emerged from the absorbers was contaminated with relatively

[10] We are indebted to A. H. Scott and C. Peterson of the Electricity Division of the National Bureau of Standards for assistance in obtaining the calibration.

[11] The magnitude of this effect was called to our attention by the article on p-p scattering at 460 Mev, by Meshcheryakov Bogachev, Neganov, and Piskarev, Doklady Akad. Nauk, S.S.S.R. 99, 995 (1954).

[12] H. A. Bethe and J. Ashkin in Experimental Nuclear Physics, edited by E. Segrè (John Wiley and Sons, Inc., New York, 1953), Vol. I.

low-energy particles, which were thought to be the cause of the discrepancies mentioned above in the shape of the $C^{12}(p,pn)C^{11}$ excitation function near 350 Mev.[2] Absorbers were placed in two positions in an attempt to measure the effect of the secondary particles. Position A was directly before the Faraday cup, so that the particles emerged from the absorber and passed through the target foils into the Faraday cup. This was essentially the technique used by Aamodt et al.[1] to degrade the proton energy. Because the $C^{12}(x,xn)C^{11}$ cross section increases for energies lower than those used in this experiment, the effect of low-energy secondary particles on the excitation function is magnified in relation to their number. Absorbers were also placed in position B, which was on the proton probe cart (Fig. 1) in the path of the scattered beam. The collimators and steering magnet then provided a good energy selector, and low-energy charged particles were no longer present in the beam entering the cave. Absorbers were also placed at position A in these experiments to obtain further energy degradation and to study the effect of the secondary particles as a function of the incident-particle energy.

Actually, several absorbers were used at position A and target foils were placed at various depths. The Faraday cup then measured the current through the last foil. To determine the current (primary plus charged secondary particles) that passed through the other foils in the absorber, separate measurements were made with an ionization chamber in front of the absorber. The same absorbers used above were than in turn inserted between the chamber and the Faraday cup to measure the fraction I/I_0 of the beam that passed through foils placed at the various depths in the absorber. This technique gave the total particle current at each foil position to an accuracy comparable with the direct measurement of the incident current, since measurements at 350 Mev with and without absorber in the beam path gave the same value for the cross section.

In analogy to the geometries defined in scattering experiments, measurements made with the absorbers at position A are referred to as "poor geometry" measurements, while those at position B are referred to as "good geometry" measurements.

C. Foils

The carbon foils were made of polystyrene, $(CH)_n$ and were 1 or 1.25 in. in diameter. The thicknesses varied from 1 to 15 mils. Some of the foils were coated with very thin layers (of the order of 100 angstroms) of silver to test the effect of nonconducting samples on the efficiency of the 4π proportional counter as described below. The aluminum foils were of the same diameters and 5 and 10 mils thick.

Each of the target foils represented a slice of a "thick" slab of the foil material. "Guard" foils of 5

TABLE I. Calculated number of high-energy electrons in the forward direction from 0.005-in. copper foil.

Particle	Effective electron range in units of extrapolated ranges		
	$1.0R_{ext}$	$0.7R_{ext}$	$0.5R_{ext}$
350-Mev proton	0.020	0.019	0.016
205-Mev proton	0.030	0.023	0.016
170-Mev proton	0.033	0.023	0.016
190-Mev deuteron	0.039	0.028	0.020
105-Mev deuteron	0.040	0.029	0.020
85-Mev deuteron	0.041	0.030	0.020
380-Mev alpha	0.13	0.092	0.067

mils thickness were placed between foils of different elements and between foils and absorbers to protect against recoil loss and capture.[13,14] In addition, several foils were usually stacked at each absorber depth, and no variation in apparent cross section was observed in these foils.

The beam diameter was 0.5 in. when the 1-inch-diameter foils were used, and 0.75 in. when the 1.25-inch-diameter foils were used. The foils were large enough to intercept essentially all the beam, including the multiply scattered portion. This was shown by inserting photographic film at each absorber depth; the blackening was always confined to an area less than that of the foils. The small fraction of the beam that may have missed the foils was compensated by the effects of the neutron contamination as shown by a beam distribution survey described in Sec. IIA.

The foils were weighed and measured to an accuracy of about 0.1%. The foils were counted for 3 or more half-lives; the C^{11} activity fitted best a 20.4-min half-life, and the Na^{24} a 15.1-hr half-life.

D. 4π Proportional Counter

The target foils were counted in a 4π constant-flow methane proportional counter.[15] A typical voltage plateau is shown in Fig. 2. No discriminator plateaus were taken because the discriminator was fixed internally at a point above the noise level. The operation of such a counter has been described by Seliger and Cavallo.[15]

Since the field is low at the sample position when nonconducting foils are counted,[15] several polystyrene foils were coated with silver to a thickness of approximately 100 angstroms (measured by the comparative light transmission of coated and uncoated foils). There was never any significant difference between the determinations of the cross section with an uncoated foil and those with a coated foil, which indicates that essentially all the β particles were energetic enough to

[13] R. E. Batzel and G. T. Seaborg, Phys. Rev. 82, 607 (1951).
[14] S. Fung and I. Perlman, Phys. Rev. 87, 623 (1952).
[15] H. H. Seliger and L. Cavallo, J. Research Natl. Bur. Standards 47, 41 (1951); also H. H. Seliger and A. Schwebel, Nucleonics 12, 54 (1954).
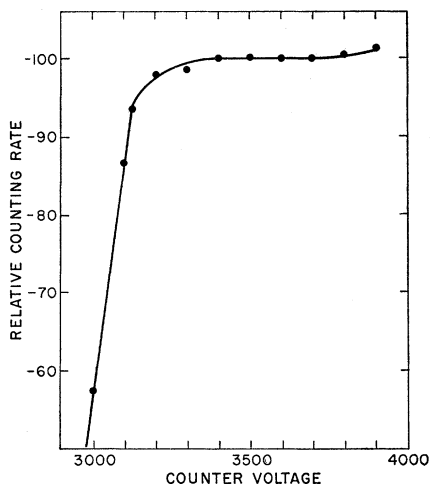
FIG. 2. Typical high-voltage plateau for the 4π proportional counter.

escape the low-field region. This problem did not enter when aluminum foils were used.

The efficiency of the counter as a function of foil diameter and foil position was also investigated. Aluminum foils varying from 0.25 to 1.5 in. in diameter were activated in a uniform neutron flux and the relative counting rate per unit weight showed no variation as a function of foil diameter within the statistical uncertainty ($\sim$1%). Also a small test foil was counted at various distances from the foil holder and no dependence on position existed in the region occupied by the foils (Fig. 3).
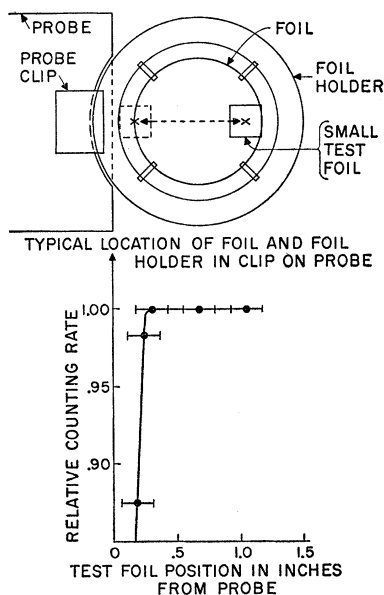

FIG. 3. The active foils were inserted into the 4π counter on a probe as shown in the figure. The geometrical sensitivity of the counter was tested with a small test foil and the relative sensitivity is shown in the lower half of the figure. The active foil was always confined to the region of uniform sensitivity.

Long-lived, β-active isotopes mounted on thin foils were used to check the performance of the counter during the period of the experiments.

To check the efficiency of the 4π counter against a suitable standard, three sources calibrated by the National Bureau of Standards were obtained.[16] Two were Tl^{204} sources and one was a $Sr^{90}-Y^{90}$ source. The sources were sandwiched between 0.2 mg/cm^2 of aluminum leaf to prevent source losses, and the NBS calibration was made after sandwiching. The ratios of the counting rates in our counter compared with those in the NBS counter were 0.99, 1.00, and 1.01; we therefore believe the counter to be 100$\pm$1% as efficient as the NBS counter, which is at least 99% efficient.[15]

E. Self-Absorption

In view of the preceding discussion, the major uncertainty in the absolute beta counting was the self-absorption in the activated foils. To determine a useful self-absorption curve required measurement of high precision, which in turn required a minimum number of measured parameters. The following factors entered into these measurements:

(1) Time between measurements should be as short as possible to minimize decay corrections.

(2) The counting rate should be as high as possible to eliminate background uncertainties.

(3) Better than 1% statistics required.

(4) Counting rate should remain almost constant to maintain dead-time correction nearly constant.

(5) The weight of the foil should not enter critically in the measurement.

(6) The uniformity of the foil activation should not enter critically into the measurement.

(7) The foil geometry should not be important.

To minimize the uncertainty from the first three factors a high counting rate was required, which aggravated the correction due to dead time. For comparing thin foils, uncertainties from factors (5) and (6) became appreciable. Two techniques were used to minimize these effects. A technique which removed most uncertainties, except factor (7), was to use a single thin foil which was counted and then folded and recounted in exactly the same counting arrangement. In this case there was a slight reduction in counting rate due to the increased thickness of the doubled foil, since the other factors remained unchanged. This procedure was repeated for increased thickness with increased uncertainties due to edge effects. To eliminate the edge effects, but with uncertainties in the dead-time corrections, uniformly activated foils were counted singly and then combined

---

[16] Courtesy of Dr. H. H. Seliger, National Bureau of Standards.

so that weighing and activation uncertainties were small.

To further reduce the uncertainties in the 4π counter measurements, the absolute disintegration of several activated foils was measured by the beta-gamma coincidence technique. In this case the activated foils were sandwiched between plastic scintillators placed on the end of a photomultiplier for the beta counting, and the gamma counting was done with a NaI scintillator. The beta efficiency was approximately 90% and the gamma efficiency roughly 3%. Slight corrections for γ-γ coincidences (0.5%) and dead-time (1%) were applied. The agreement between 4π counting and the β-γ counting was good, but in the case of the polystyrene foils the β-γ point appeared to be slightly higher than the extrapolation of the 4π counting data to zero thickness. Since both measurements have systematic uncertainties of the order of this difference,
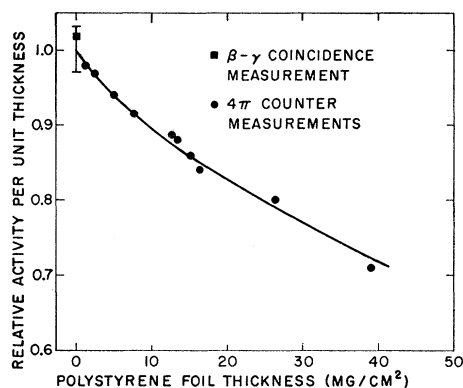

FIG. 4. The fraction of the C^{11} decay positrons escaping from a uniformly activated polystyrene is plotted against the foil thickness. The curve is arbitrarily normalized to the mean value of the β-γ coincidence measurement and the extrapolation of the 4π measurements to zero thickness.

the self-absorption curves were normalized to a point midway between the two zero-point determinations.

The self-absorption curve for uniformly activated polystyrene is shown in Fig. 4. The curve should apply to any measurement of the C^{11} activity in foils where the activated area is more than a range of the beta particles from the foil edge. In high-energy bombardment, the production of Be^7 in the foil requires that the foils be counted less than 2.5 hours after bombardment for the contaminating activity from Be^7 to be less than 1% The similar curve for Na^{24} activity in aluminum is shown in Fig. 5. In this case contamination by F^{18} and Na^{22} require that the measurements be made more than 18 hours but less than 3.5 days after bombardment to be free from contaminating activity. In particular, the Na^{22} activity, with its low-energy betas, has a much steeper self-absorption curve and can produce large uncertainties in the measurements.
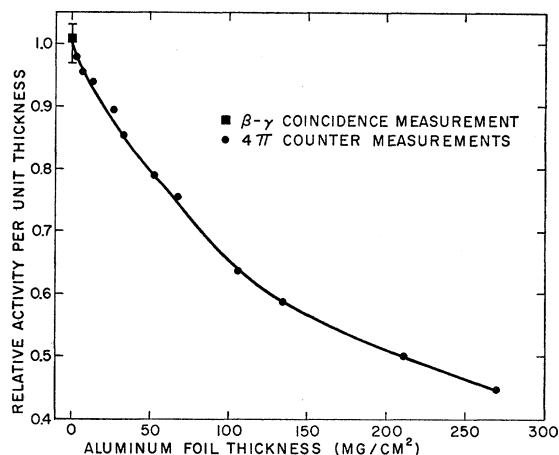

FIG. 5. The fraction of the Na^{24} decay betas escaping from a uniformly activated aluminum foil is plotted against the foil thickness. The curve is arbitrarily normalized to the mean value of the β-γ coincidence measurement and the extrapolation of the 4π measurements to zero thickness.

III. RESULTS

A. Energy Dependence of Cross Sections

The measurements of the $C^{12}(x,xn)C^{11}$ cross sections as a function of energy showed a significant dependence on the position of the absorber in relation to the target foil. Measurements made in "poor geometry" (position A) consistently gave apparent cross sections about 7% higher than those measured in "good geometry" (position B). This dependence was ascribed to the charged and uncharged secondary particles that leave the absorber. (A crude calculation of the effects agreed very well with the empirical corrections.)

Figure 6 shows the apparent variation of the $C^{12}(p,pn)C^{11}$ cross section as a function of the proton

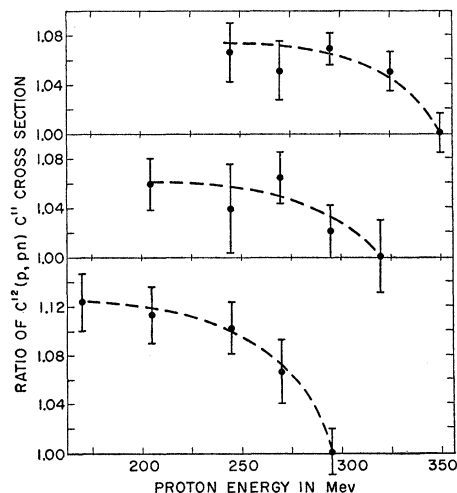
FIG. 6. The apparent $C^{12}(p,pn)C^{11}$ cross section from "poor geometry" measurements is plotted against proton energy for three different incident proton energies. The apparent rise at lower energies is due to secondary interactions in the attenuator (see text).
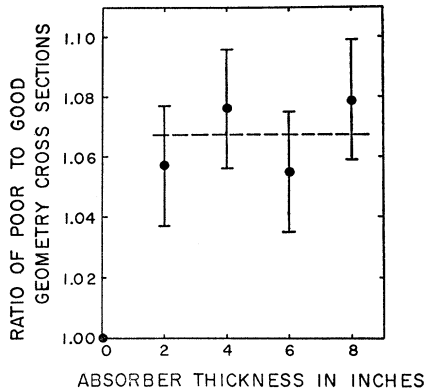
FIG. 7. The apparent increase in the $C^{12}(p,pn)C^{11}$ cross section due to secondary interactions is plotted *versus* absorber thickness in the "poor geometry" measurements.

energy. Measurements for three different incident beam energies are shown (the incident energy was varied by placing absorbers in position B, and the variation of the cross section with energy was determined by placing absorbers in position A). In each case the cross sections are normalized to the value at the incident beam energy. All the curves show the rise found in earlier experiments,[1] and it would appear that the increase is a consequence of the method of beam degradation rather than a true nuclear effect, for the cross section for the "good geometry" measurements is essentially constant.

The ratio of the apparent cross section as a function of absorber thickness is shown in Fig. 7. The points are an average of the data shown in Fig. 6, with the lowest-energy point (170 Mev) omitted (since at this energy the cross section appears to show a significant increase). The conclusion drawn from Fig. 7 is that the secondary particles increase the observed cross section in a constant ratio for absorbers greater than a given thickness. The effect of the secondaries does not continue to increase as the absorber thickness increases because

(1) the low-energy secondary particles are scattered, and a fraction, which increases with absorber thickness, misses the foil;

(2) the relatively low-energy charged secondary particles are removed by ionization loss within a short distance from their creation; and

(3) the secondary particles are emitted with an angular distribution so that a large fraction of those formed in the front of the absorber miss the foil.

The results of these measurements would seem to remove the discrepancy mentioned in the introduction in the shape of the excitation function, and would require that the excitation function reported in reference 1 be corrected for energies below the maximum beam energy.

Similar behavior is exhibited by the $C^{12}(d,dn)C^{11}$

excitation function, although the details are different because deuteron and proton interactions give different energy and angular distributions for the secondary particles.

The excitation function for $C^{12}(\alpha,\alpha n)C^{11}$ was not measured, but somewhat similar behavior probably should be expected.

A. Absolute Values of the Cross Sections

The absolute values of the cross sections were calculated from the formula

$$\sigma = \frac{A_{00}}{\lambda} \frac{1}{N} \frac{A}{A_{0}t},$$

where A_{00}/λ is the number of reactions produced by N particles in a foil with $A_{0}t/A$ nuclei per unit area. The last quantity was calculated from the measured weights and diameters of the foils; the first, from the decay constant λ and the measured counting rates corrected for decay and self-absorption; the second, from the charge collected by the Faraday cup corrected for high-energy electrons. No correction was applied for neutron-induced events and the fraction of the beam collected by the Faraday cup that missed the foils, because these two effects cancelled each other. The cross sections measured in "poor geometry" were corrected by the empirically determined factors for the effects of secondary particles; for protons the correction was a uniform reduction of $1/1.07$; for deuterons, a reduction of $1/1.04$ for 0.5-in. carbon absorbers and $1/1.08$ for greater thicknesses. The correction may be significantly in error for the lower deuteron energies because the absorbers were relatively thick compared with the ranges. All energy measurements were based on the Aron et al.[17] range curves. None of the cross sections was corrected for the isotopic abundance.

As an additional check on the beam-monitoring technique, the $C^{12}(p,pn)C^{11}$ cross section was measured for 340-Mev protons by bombarding $1\times1\times0.75$-in. plastic scintillator (effectively polystyrene) in a uniform proton flux. Ilford G.5 emulstions were placed on each side of the scintillator and proton tracks were counted to determine the particle flux. The C^{11} activity was counted by placing the scintillator in optical contact with a photomultiplier tube and the counting efficiency was determined by the β-γ coincidence technique. This measurement gave a cross section of 36 ± 3 mb.

The ratio of the $C^{12}(p,pn)C^{11}$ and $Al^{27}(p,3pn)Na^{24}$ cross sections was measured by the simultaneous bombardment of a sandwich of aluminum and polystyrene foils at 340 Mev and was found to be 3.21, in agreement with the ratio of the absolute cross sections determined independently.

[17] Aron, Hoffman, and Williams, Atomic Energy Commission Report AECU-663 (unpublished).

C. Errors

The absolute cross sections are listed in Table II with their associated relative standard errors. The values quoted are subject to various systematic errors, some of which have been discussed above. They include

(1)	self-absorption	$\pm 3\%$
(2)	condenser and electrometer calibration	$<\pm 1\%$
(3)	counter efficiency	$+1\%$
(4)	secondary particle effect	$\pm 2\%$
(5)	knock-on electrons	± 1 to $\pm 4\%$ (Table I)
(6)	beam spatial distribution	$+1.25\%$
(7)	neutron contamination	-1.25%
(8)	half-life uncertainty	$<\pm 1\%$

An estimate of the accuracy of our measurements is $+5$ and -4% for 350-Mev protons and 190-Mev deuterons.

D. Comparison with Other Measurements

Also listed in Table II are results of previously published values of the absolute cross sections. With the exception of the $C^{12}(p,pn)C^{11}$ cross section, all our values are as much as 20% larger than those previously reported. Full discussions of the techniques and corrections applied to these measurements were not

TABLE II. Absolute reaction cross sections (4π counter data only).

	Particle energy (Mev)	Geometry	Cross section[a] (mb)
A. $C^{12}(p,pn)C^{11}$	350	good	36.0±0.7
	320	good	35.5±0.7
	325	poor	35.9±0.8
	295	good	37.9±0.4
	295	poor	35.5±1.0
	270	poor	35.9±1.0
	240	poor	37.2±1.8
	204	poor	37.0±2.0
	170	poor	39.7±0.9
B. $C^{12}(d,dn)C^{11}$	190	good	61.1±0.6
	180	good	60.8±0.6
	180	poor	60.6±1.3
	160	good	60.6±0.9
	160	poor	61.3±1.3
	145	poor	60.6±1.8
	130	poor	61.6±1.8
	105	poor	60.7±1.0
	85	poor	56.9±1.8
C. $C^{12}(\alpha,\alpha n)C^{11}$	380	good	57.0±0.6
	380	good	48 ±3[b]
D. $Al^{27}(p,3pn)Na^{24}$	350	good	11.1±0.2
	420	...	10.8±0.5[c]
E. $Al^{27}(d,3p2n)Na^{24}$	190	good	28.8±0.3
	190	good	22 ±2[d]
F. $Al^{27}(\alpha,4p3n)Na^{24}$	380	good	24.2±0.3
	380	good	23.4[b]

[a] Note: All errors are standard errors of a single measurement and do not include estimated uncertainties due to possible systematic effects. Corrections for self-absorption, geometry, and knock-on electrons have been made. See text.
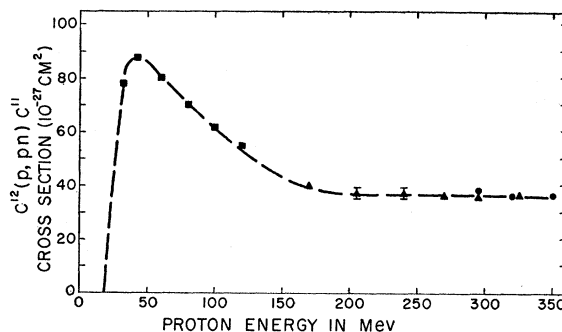[b] See reference 3.
[c] See reference 6.
[d] See reference 5.

FIG. 8. The excitation function for the $C^{12}(p,pn)C^{11}$ reaction is plotted as a function of proton energy. The dots are "good geometry" measurements, and the triangles are "poor geometry" measurements, corrected as described in the text. The squares are from the data of reference 1 normalized to 36.0 mb at 350 Mev.

given, so it is difficult to assess the severity of the discrepancies. It should be noted that essentially the same beam-monitoring techniques were used in all the experiments, and that corrections for the knock-on electrons from the Faraday cup housing foil were not applied to the previous measurements.

Recently Rosenfeld et al.[18] have redetermined the $C^{12}(p,pn)C^{11}$ cross section at 460 Mev and quote 33 mb as a preliminary value, in reasonable agreement with our results. Also recent measurements up to 2.9 Bev[19] of the ratio of the $C^{12}(p,pn)C^{11}$ and $Al^{27}(p,3pn)Na^{24}$ cross sections are in reasonable agreement with our results.

The most significant difference from earlier experiments is the shape of the $C^{12}(p,pn)C^{11}$ excitation curve in the neighborhood of 350 Mev (Fig. 8). Readjusting the excitation function both in shape and absolute value will have important effects on seemingly unrelated experiments because of the widespread use of the reaction as a beam monitor. For example, the p-p scattering cross sections measured at 240 Mev by Oxley et al.[8] should certainly be modified. Even though they intercalibrated their counter with a beta standard used by Aamodt et al., the revised shape of the excitation function requires a 41/49 reduction in their values (to 4.05±0.32 mb/sterad). If a cross section of 36.0 mb for the $C^{12}(p,pn)C^{11}$ reaction is used, their values are further reduced (to 3.56±0.28 mb/sterad) and are in excellent agreement with the results of Chamberlain et al.[20] (3.6±0.2 mb/sterad).

The p-p scattering cross sections measured by Birge et al.[8] at 105 and 75 Mev may be reduced directly by the ratio 36/41 (to 4.8±0.9 and 5.8±1.2 mb/sterad, respectively). The revised values are in agreement with the Berkeley measurements.[20]

Cassels et al.[8] measured the p-p scattering cross sections at 146 Mev by using two methods to calibrate

[18] A. H. Rosenfeld (private communication).
[19] R. F. Wolfgang and G. Friedlander, Phys. Rev. 96, 190 (1954); and erratum (to be published).
[20] Chamberlain, Segrè, and Wiegand, Phys. Rev. 83, 932 (1951).
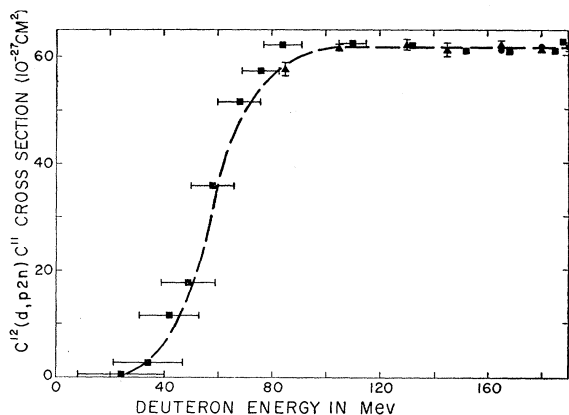
FIG. 9. The excitation function for the $C^{12}(d,dn)C^{11}$ reaction is plotted as a function of the deuteron energy. The dots are "good geometry" measurements, and the triangles are "poor geometry" measurements, corrected as described in the text. The squares are the end-window counter data normalized at 190 Mev to the 4π counter data.

their beam monitor. One of the methods involved the use of the $C^{12}(p,pn)C^{11}$ cross section and gave a p-p scattering cross section of 4.61 ± 0.55 mb/sterad. This result should be reduced in the ratio 43/57 to 3.56 ± 0.42 mb/sterad. Their value based on a photographic emulsion calibration remains high compared with other measurements.

E. End-Window Counter Measurements

The stacked-foil technique was used to measure the relative excitation functions of deuterons and He^3 particles for the $C^{12}(x,xn)C^{11}$ reaction. Graphite foils $1\frac{11}{16}$ in. in diameter and $\frac{1}{8}$ and $\frac{1}{16}$ in. thick were placed between guard foils and inserted at various depths in uranium absorbers. Near the end of the range, the carbon foils were inserted consecutively. The incident-particle current was measured by an ionization chamber and the current through each foil was determined from charge-attenuation curves measured with a Faraday cup.[21]

The foils were counted in an end-window β counter with a 3.5-mg/cm^2 window. The counter and its use in connection with these experiments are described more fully in a paper by Schecter et al.[22] No activity other than the 20.4-minute C^{11} was observed; the foils were counted for several half-lives. Corrections were applied for counter dead time, C^{11} decay, and geometry differences (found empirically).

The excitation curve for deuterons was normalized to the high-energy point from 4π counter data, and the low-energy cross sections were corrected for secondary particles as in Sec. IIB. The range of the deuterons was

[21] Millburn, Birnbaum, Crandall, and Schecter, Phys. Rev. 95, 1268 (1954), and unpublished data.
[22] Schecter, Crandall, Millburn, and Ise, Jr., Phys. Rev. 97, 184 (1955).
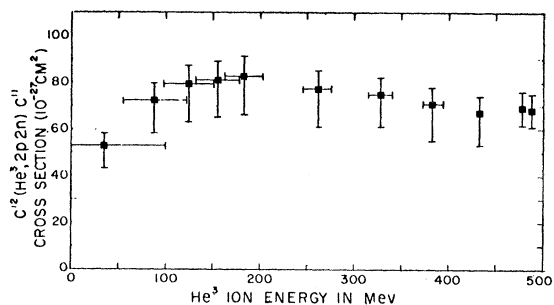

FIG. 10. The excitation function of the $C^{12}(He^3,He^3n)C^{11}$ reaction is plotted as a function of the He^3 energy. The measurements were made with an end-window counter whose efficiency was determined relative to the 4π counter through the normalization of the 190-Mev deuteron data. The correction for secondary interactions at less than the maximum energy is very uncertain and is reflected in the unsymmetrical errors.

determined for a similar stack and the energies were computed from the tables of Aron et al.[17] Uncertainties in the range point cause the large energy uncertainties for low energies; the horizontal lines in Fig. 9 represene an estimate of the uncertainty in placement of tht midpoint, and do not represent merely the spread (due to range straggling) of energies that pass through the foil.

The excitation function for He^3 particles shown in Fig. 10 was normalized on the basis of the deuteron data, because both curves were measured under the same experimental conditions. The techniques and corrections were the same for both cases; for the cross sections shown in Fig. 10, a constant correction of $1/1.08$ was applied to the data for energies lower than the maximum. The errors on the points are unsymmetrical because it was felt that such a correction for secondary-particle effects was very likely incorrect for incident He^3 particles. The inelastic and stripping cross sections for He^3 are approximately equal to those for deuterons,[21] but the stripped secondaries have ranges greater than the residual range of the He^3 particle.[20] Thus the effects of the secondary particles may not level off to a constant value as quickly as they do for protons and deuterons whose secondaries have ranges shorter than the residual range of the primary particle. Caution should be exercised in use of the data of Fig. 10, for the measured shape of the excitation function may be incorrect. The cross section is constant within experimental error for energies greater than 80 Mev.

IV. SUMMARY AND CONCLUSIONS

In addition to obtaining absolute values of the cross sections, we have measured the ratios of the various reaction cross sections with a good degree of accuracy, certainly to less than 5%. In addition we have shown that the $C^{12}(x,xn)C^{11}$ excitation functions are nearly constant at and near the maximum energies of the charged-particles beams available at Berkeley; earlier measurements that indicated a sharp dip near the

maximum energy underestimated the effect of secondary particles produced in the attenuators.

The absolute value of the $C^{12}(p,pn)C^{11}$ cross section at 350 Mev is significantly lower than that reported earlier,[1] and the difference is believed to be due to the increased accuracy of absolute β counting that has been achieved in the last few years. Readjustment of the excitation function on the basis of our results leads to improved agreement between the p-p scattering cross sections measured at Berkeley and those measured elsewhere[8] using the $C^{12}(p,pn)C^{11}$ reaction to monitor the proton beam. The reported results of other experiments will be affected by the readjustment of the

excitation function; a partial list of such experiments is given in references 6 to 8.

ACKNOWLEDGMENTS

Production of Deuterons in High-Energy Nucleon Bombardment of Nuclei and Its Bearing on Nuclear Charge Distribution

Wilmot N. Hess and Burton J. Moyer
Radiation Laboratory, University of California, Berkeley, California
(Received August 2, 1955)

A study has been made of deuterons produced at wide angles to a beam of 300-Mev neutrons and a beam of 300-Mev protons. The cross-section dependence on atomic number for these deuterons for light elements can be written as $\sigma = kA^{1.2}$. This fact and the energy spectra and angular distribution of the deuterons show that the process that forms these deuterons is related to the indirect pick-up process described by Bransden. This is a two-step process in which the incident nucleon, or its collision partner, is scattered and then picks up a deuteron-forming partner in the same nucleus. A yield of tritons has also been observed which has the same A-dependence and is presumably made by a similar process. The A-dependence of the deuteron-production cross section also suggests that these deuterons are made on the nuclear surface. Because of this A dependence, a comparison of the deuteron yields using an incident neutron beam and an incident proton beam can give information about the relative numbers of neutrons and protons on the surface of the nucleus. An analysis of this sort leads to a possible conclusion that for heavy nuclei there is a nuclear skin rich in neutrons. For light nuclei the effect is not observed. If this skin is composed only of neutrons its thickness must be about 0.8×10^{-13} cm for lead.

I. INTRODUCTION

AMONG the various phenomena that reveal the constitution and organization of the nucleus are the identity and characteristics of the secondary particles that emerge under controlled bombarding conditions. The deuteron as a secondary particle has been of considerable interest, since its small binding energy invites questions as to the processes by which it may emerge intact, particularly in high-energy events. The elucidation of these phenomena has contributed to the "pick-up" concepts which have been prominent in recent nuclear reaction theory.

In 1952, at this laboratory, Clark[1] observed a yield of deuterons at 40° to a 340-Mev proton beam from a carbon target. Because these deuterons were made at a large angle to a high-energy beam, it was improbable that they were direct pick-up deuterons.[2,3] Because of

the way they are formed, direct pick-up deuterons are quite sharply peaked along the direction of the beam, and have energies fairly closely related to the beam energy. It is expected that there will be considerably fewer direct pickup deuterons at 340 Mev than at 100 Mev. At about the time Clark first observed these deuterons, Bransden[4] wrote a theoretical paper describing a method for producing deuterons of characteristics similar to those observed. Quoting from Bransden's paper, "Deuterons may be formed as the result of a second-order process in which a nucleon of relatively small momentum (produced by the collision of the incident neutron with a nucleon in the target nucleus) picks up a second nucleon in the target nucleus to form a deuteron."

This mechanism of formation could account for the observed deuterons. It is known that the energy spectrum of protons quasi-elastically scattered from carbon at 40° from a 340-Mev proton beam shows a character-

[1] D. D. Clark (private communication).
[2] J. Hadley and H. York, Phys. Rev. **80**, 345 (1950).
[3] G. F. Chew and M. L. Goldberger, Phys. Rev. **77**, 470 (1950).
[4] B. H. Bransden, Proc. Phys. Soc. (London) **A65**, 738 (1952); and private communication.